



Neutrophil-activating secretome characterizes palbociclib-induced senescence of breast cancer cells

Gabriele Favaretto¹ · Marianna Nicoletta Rossi² · Lorenzo Cuollo^{3,6} · Mattia Laffranchi³ ·
Manuela Cervelli² · Alessandra Soriani³ · Silvano Sozzani^{3,4,5} · Angela Santoni^{3,4,5} · Fabrizio Antonangeli¹

Received: 27 November 2023 / Accepted: 30 March 2024 / Published online: 2 May 2024
© The Author(s) 2024

Abstract

Senescent cells have a profound impact on the surrounding microenvironment through the secretion of numerous bioactive molecules and inflammatory factors. The induction of therapy-induced senescence by anticancer drugs is known, but how senescent tumor cells influence the tumor immune landscape, particularly neutrophil activity, is still unclear. In this study, we investigate the induction of cellular senescence in breast cancer cells and the subsequent immunomodulatory effects on neutrophils using the CDK4/6 inhibitor palbociclib, which is approved for the treatment of breast cancer and is under intense investigation for additional malignancies. Our research demonstrates that palbociclib induces a reversible form of senescence endowed with an inflammatory secretome capable of recruiting and activating neutrophils, in part through the action of interleukin-8 and acute-phase serum amyloid A1. The activation of neutrophils is accompanied by the release of neutrophil extracellular trap and the phagocytic removal of senescent tumor cells. These findings may be relevant for the success of cancer therapy as neutrophils, and neutrophil-driven inflammation can differently affect tumor progression. Our results reveal that neutrophils, as already demonstrated for macrophages and natural killer cells, can be recruited and engaged by senescent tumor cells to participate in their clearance. Understanding the interplay between senescent cells and neutrophils may lead to innovative strategies to cope with chronic or tumor-associated inflammation.

Keywords Breast cancer · Palbociclib · Senescence · SASP · Serum amyloid A · Neutrophil · NET

Gabriele Favaretto and Marianna Nicoletta Rossi have contributed equally.

✉ Fabrizio Antonangeli
fabrizio.antonangeli@cnr.it

Gabriele Favaretto
gabriele.favaretto@cnr.it

Marianna Nicoletta Rossi
mariannanicoletta.rossi@uniroma3.it

Lorenzo Cuollo
lorenzo.cuollo@uniroma1.it

Mattia Laffranchi
mattia.laffranchi@uniroma1.it

Manuela Cervelli
manuela.cervelli@uniroma3.it

Alessandra Soriani
alessandra.soriani@uniroma1.it

Silvano Sozzani
silvano.sozzani@uniroma1.it

Angela Santoni
angela.santoni@uniroma1.it

Abbreviations

ANCA	Antineutrophil cytoplasmic antibody
DAMP	Damage-associated molecular pattern
EMT	Epithelial-to-mesenchymal transition

¹ Institute of Molecular Biology and Pathology (IBPM), National Research Council (CNR), c/o Department of Molecular Medicine, Sapienza University of Rome, Viale Regina Elena 291, 00161 Rome, Italy

² Department of Science, Roma Tre University, Rome, Italy

³ Department of Molecular Medicine, Sapienza University of Rome, Rome, Italy

⁴ Istituto Pasteur Italia-Fondazione Cenci Bolognetti, Rome, Italy

⁵ IRCCS Neuromed, Pozzilli, Italy

⁶ Present Address: Department of Pediatrics, Columbia University, New York, NY, USA

FDA	Food and Drug Administration
IL-8	Interleukin-8
LPS	Lipopolysaccharide
mAb	Monoclonal antibody
MDSC	Myeloid-derived suppressor cell
MFI	Median fluorescence intensity
MPO	Myeloperoxidase
NET	Neutrophil extracellular trap
NK	Natural killer
PMA	Phorbol 12-myristate 13-acetate
ROS	Reactive oxygen species
SA- β -Gal	Senescence-associated β -galactosidase
SAA	Acute-phase serum amyloid A
SASP	Senescence-associated secretory phenotype
TAN	Tumor-associated neutrophil
TIS	Therapy-induced senescence

Introduction

Cellular senescence represents a cellular stress response primarily triggered by DNA damage, including telomere shortening and cytosolic nucleic acid sensing, and it is considered an alternative fate to regulated cell death [1–3]. Senescent cells are characterized by a long-lasting cell cycle arrest and therefore are regarded as a hurdle against tumorigenesis [4]. Nevertheless, senescent cells are metabolically active and many of their biological functions are driven by the so-called senescence-associated secretory phenotype (SASP). This is a complex and temporally regulated program that involves the secretion of bioactive molecules and inflammatory factors in the surrounding microenvironment [5–7]. SASP makes senescent cells crucial in orchestrating immune cell recruitment and tissue plasticity around neoplastic lesions, showing even opposite effects on tumor progression [8]. For instance, senescence-dependent recruitment of lymphocytes of the innate immunity, namely natural killer (NK) cells, can mediate tumor regression [9–11]. NK cells recognize senescent cells expressing the ligands of the activating receptors NKG2D and DNAM-1 and eliminate them through the release of perforin- and granzyme-containing granules [12–16]. Macrophages also participate in the clearance of senescent cells [17, 18]. Furthermore, senescent cells have been recently described to alert the adaptive arm of the immune system by enhancing tumor cell immunogenicity through the priming of dendritic cells and the activation of tumor antigen-specific CD8 T cells [19, 20]. On the other hand, senescence can also establish an immunosuppressive microenvironment [21] and promote cancer cell stemness [22]. In certain contexts, senescent cells may express the inhibitory molecule HLA-E, dampening NK cell, and CD8 T cell effector functions [23], and expand the myeloid-derived suppressor cell (MDSC) compartment

within the tumor niche [24]. Much less is known about the interaction between senescent cells and neutrophils, which are the first immune cells recruited to injured tissues. Neutrophils have been reported to target senescent cells during vascular remodeling in retinopathy [25] and to be influenced by the secretome of senescent hepatoma cells with contrasting results on neutrophil extracellular trap (NET) formation capacity [26]. Considering the increasing evidence of a prominent role of neutrophils in the tumor immune landscape, there is an urgent need to investigate the cross talk between senescent cells and neutrophils. According to the state of the art, tumor-associated neutrophils (TANs) can establish antitumor responses by direct killing of cancer cells via reactive oxygen species (ROS) production or by serving as antigen-presenting cells. Conversely, TANs can skew the immune responses toward a tumor-promoting inflammation and a permissive environment driving angiogenesis and extracellular matrix remodeling [27].

Immunotherapy has revolutionized cancer treatment and the therapeutic efficacy of many anticancer drugs relies on their immunomodulatory effects [28, 29]. Cellular senescence has great potential as an immunomodulatory tool due to its intimate connection with the immune system. Pro-senescence therapy of tumor cells may even be considered as a new type of immunotherapy [30]. Palbociclib (PD0332991), ribociclib (LEE011), and abemaciclib (LY2835219) belong to the third generation of CDK4/6 inhibitors, which have been recently approved in association with hormonal therapy for the treatment of hormone receptor-positive and human epidermal growth factor receptor 2-negative (HR +/HER2-) metastatic breast cancer and have promptly demonstrated additional effects beyond the antiproliferative property [31–33]. Palbociclib (Ibrance, Pfizer Inc.), the first licensed, has shown non-canonical functions among which the induction of a senescence-like phenotype in tumor cells has attracted great attention for its implications in cancer pathology [34–37]. In this regard, palbociclib treatment may represent a form of therapy-induced senescence (TIS). Preclinical evidence extends palbociclib application also to tumors other than breast cancer, including leukemias, melanoma, pancreatic carcinoma, head and neck cancer, and glioblastoma [38–40]. Moreover, palbociclib is being tested in clinical trials in combination with immune checkpoint inhibitors or other agents [41, 42]. Noteworthy, a recent alert from the Food and Drug Administration (FDA) warns about severe pulmonary adverse effects following the administration of CDK4/6 inhibitors, including palbociclib, and a preclinical study has shown that palbociclib treatment leads to neutrophil recruitment to fibrotic lung lesions potentially contributing to pulmonary inflammation [43, 44]. Therefore, shedding light on the way palbociclib-induced senescent cells modulate neutrophil behavior is of great relevance. To this aim, in this work we treated human

breast cancer cells with palbociclib to study the induction of cellular senescence and to analyze the resulting SASP. Specifically, we assessed the ability of senescent tumor cells to mediate inflammation by recruiting and activating neutrophils.

Materials and methods

Cell culture and treatment

Human breast cancer cell lines MCF7 and MDA-MB-231 were kindly gifted by Rossella Maione (Sapienza University of Rome, Italy). Primary human foreskin fibroblasts (HFFs) were from the American Type Culture Collection, ATCC SCRC-1041™. Cells were routinely screened for mycoplasma contamination with the PCR mycoplasma detection kit from abm (G238). Cells were cultured in a humidified incubator at 37°C with 5% CO₂ in DMEM high glucose supplemented with 10% FBS, 2 mM L-Gln, and 100 U/ml penicillin/streptomycin (Euroclone). Optimal seeding density was established for each cell line to reach 70–80% confluence at the experimental endpoint. Palbociclib (PD0332991) was provided by Pfizer Inc. and used at 2 μM which is a standard concentration in cellular studies [45] and not far from physiologically achievable concentrations in the plasma of patients [46].

Cell cycle analysis

Cells were harvested and fixed in cold 70% ethanol at least overnight at 4°C. After washing in PBS, cells were incubated with 50 μg/ml propidium iodide containing 40 μg/ml RNase A for 30 min at room temperature and immediately analyzed by flow cytometry with a CytoFLEX cytometer from Beckman Coulter. Data were elaborated using FlowJo software v.10.7.1 (FlowJo, OR, USA), and cell cycle determined with the Dean-Jett-Fox model after doublets exclusion.

Apoptosis evaluation

Apoptotic and dead cells were detected using the dead cell apoptosis kit with Annexin V FITC and propidium iodide for flow cytometry from Invitrogen (V13242) according to the manufacturer's instructions.

SA-β-Gal assay

Senescence-associated β-galactosidase (SA-β-Gal) activity was assessed by using the senescence β-galactosidase staining kit from cell signaling technology (#9860) according to the manufacturer's instructions. Senescent cells were

identified as blue-stained cells by standard light microscopy. Images were acquired using an EVOS microscope with magnification 200×.

Lamin-B1 detection

Lamin-B1 was detected by immunofluorescence microscopy. Cells were fixed with methanol/acetone at ratio 3/7 and stained overnight at 4°C with anti-Lamin-B1 rabbit mAb (Abcam, ab133741) diluted 1:100 in PBS with 5% BSA, 0.3 M glycine, 0.1% Triton X-100. After washing in PBS, AF594-cojugated goat anti-rabbit IgG secondary antibody (Invitrogen, A-11012) was applied for 1 h at room temperature. Cover slip was mounted using SlowFade™ gold antifade mountant with DAPI (Invitrogen, S36938). Images were acquired by conventional epifluorescence microscopy using an Olympus BX51 microscope equipped with a ProgRes® MF cool monochrome camera (Jenoptik) and processed with I.A.S software ver. 009 (Delta Sistemi) for merging and pseudo-coloring adjustment.

Conditioned medium collection

At the end of the treatment, culture medium containing FBS was replaced with fresh medium without FBS. Treated and untreated cells were cultured in T-25 flasks with 6 ml of medium and, after 24 h, conditioned media were collected, and cells counted. Supernatants were centrifuged (13,000 rpm for 15 min at 4°C) to remove cell debris and stored unconcentrated in aliquots at –80°C until the day of use. Media were thawed on ice and used undiluted, 100 μl for ELISA analysis and 0.5 ml in 24-well plate for neutrophil functional assays.

Luminex multiplex immunoassay

Cytokine levels in cell culture supernatants were measured using a custom human premixed multi-analyte kit (R&D Systems) and a Bio-Plex® MAGPIX™ multiplex reader (Bio-Rad Laboratories) according to the manufacturer's instructions. Levels of CCL2, CCL27, CCL3, CCL4, CCL7, Chemerin, CX₃CL1, CXCL10, CXCL9, GM-CSF, IFN-γ, IL-10, IL-12, IL-13, IL-15, IL-18, IL-1α, IL-1β, IL-2, IL-21, IL-28A, IL-4, IL-5 were measured. Samples were run in duplicate and cytokine concentrations were calculated using a six-point standard curve derived from measurement of serially diluted panel-specific standards. Upper and lower limits of detection for each cytokine were based on individual analyte standard curve.

IL-6, IL-8, and SAA1 ELISA

Centrifugation-cleared cell culture supernatants were stored at -80°C until the day of analysis. IL-6, IL-8/CXCL8, and SAA1 concentrations were quantified using specific Duo-Set® ELISA Kits (R&D Systems, DY206-05, DY208-05, and DY3019-05, respectively) according to the manufacturer's instructions. Concentrations were normalized to the number of cells counted immediately after supernatant collection.

Gene expression analysis by quantitative real-time PCR (qPCR)

Total RNA was extracted using the TRIzol™ Reagent (Invitrogen, #15596026), and cDNAs were obtained using the SuperScript Vilo kit (Invitrogen, #11754050) according to the manufacturer's instructions. For the targets *CXCL1* (Hs00236937_m1), *CXCL8* (Hs00174103_m1), *SAA1* (Hs07291672_g1), and *SAA2* (Hs01667582_m1), qPCR assays were performed using TaqMan Universal PCR Master Mix (#4369016) and gene expression assays from Applied Biosystems. Gene expression was normalized using *HPRT1* (Hs02800695_m1) as housekeeping gene. For the targets *CXCL5*, *CXCL6*, and *CXCL7*, qPCR assays were performed using SsoAdvanced Universal SYBR Green Supermix (Bio-Rad Laboratories, #1725271). *GAPDH* was used as housekeeping gene. Specific primer sets were used, and primers sequences are available upon request. Reactions were performed using an AriaMx 3005 Real-Time PCR System (Agilent Technologies). Data were analyzed with the $2^{-\Delta\Delta\text{Ct}}$ method using the average of control samples for the $\Delta\Delta$ calculation.

Neutrophils isolation

Neutrophils were isolated from peripheral blood of healthy donors according to [47]. Briefly, pellet obtained from density gradient centrifugation as for peripheral blood mononuclear cell (PBMC) preparation containing polymorphonuclear cells were subjected to several steps of red blood cell lysis with buffer containing 0.155 M NH_4Cl , 12 mM NaHCO_3 , and 0.1 mM EDTA. Polymorphonuclear cells were resuspended in PBS and counted. For the analysis of viability and purity, a small amount of isolated polymorphonuclear cells (0.2×10^6 cells) were stained with Zombie Violet™ Fixable Viability Dye (BioLegend, #423114) and then with FITC-conjugated anti-CD10 mAb (BD Biosciences, #347503), APC-conjugated anti-CD15 mAb (Immunotools, #21890156), and PE-conjugated anti-CD16 mAb (BD Biosciences, #332779). Samples were analyzed by

flow cytometry with a CytoFLEX cytometer from Beckman Coulter, and data elaborated using FlowJo software v.10.7.1 (FlowJo, OR, USA). Gating strategy to identify neutrophils is shown in Supplementary Fig. 2.

Neutrophil migration assay

Migration of fresh isolated neutrophils was assessed in transwells (24 wells/plate) with inserts made of 3 mm-pore membrane (Corning Costar, #3415). The lower chamber was loaded with 600 μl of attracting medium according to the experimental design, while 0.5×10^6 neutrophils were loaded in the upper chamber with 100 μl . Migration assay was performed in the absence or presence of 1 $\mu\text{g}/\text{ml}$ neutralizing α -human CXCL8 mAb (R&D Systems, MAB208) placed both in the upper and lower chambers. After 1 h at 37°C , the number of neutrophils migrated across the filter into the lower chamber was counted by flow cytometry with a CytoFLEX cytometer from Beckman Coulter, and data shown as percentage of migrated neutrophils in respect of loaded neutrophils.

Neutrophil phenotyping

Cell morphology, NET formation, and ROS production were addressed after incubating 10^5 fresh isolated neutrophils for 1 h at 37°C with conditioned media according to the experimental design. For circularity evaluation, neutrophils were fixed in 4% PFA, permeabilized with 0.2% Triton X-100, stained with AF594-conjugated phalloidin (Thermo Fisher Scientific, A12381), and counterstained with 2 $\mu\text{g}/\text{ml}$ Hoechst-33342 (Thermo Fisher Scientific, H3570). Images were acquired by conventional epifluorescence microscopy using an Olympus BX51 microscope equipped with a ProgRes® MF cool monochrome camera (Jenoptik) and processed with I.A.S software ver. 009 (Delta Sistemi) for merging and pseudo-coloring adjustment. Cell circularity score was measured using the ImageJ image analysis software (Rasband, W.S., ImageJ, U. S. National Institutes of Health, Bethesda, Maryland, USA, <https://imagej.nih.gov/ij/>, 1997–2018) analyzing for each experimental condition 200 cells from 5 different fields acquired from two independent experiments. Briefly, images at $400\times$ magnification were processed performing the following actions: subtract background, adjust threshold, fill holes, analyze particles. The “overlay mask” was considered for visualizing results and the “round parameter” was considered for roundness index quantification. NETs were visualized by extracellular DNA staining with NucGreen™ Dead 488 ReadyProbes™ Reagent (SYTOX™ Green) (Invitrogen, R37109), a fluorescent membrane-impermeable DNA dye, according to the manufacturer's instructions. Cells were counterstained with 2 $\mu\text{g}/\text{ml}$ Hoechst-33342 (Thermo Fisher Scientific, H3570).

When indicated (ctr+), neutrophils were stimulated with 50 ng/ml PMA (Sigma-Aldrich, P1585) for 1 h to induce NET formation. Medium alone with FBS was used for basal background (ctr-). Images were captured by fluorescence microscopy as described above. CellROX® Green Reagent from Invitrogen (C10444) was used to estimate intracellular ROS according to the manufacturer's instructions. Neutrophils were treated with 1 µg/ml LPS (InvivoGen, TLR-EBLPS) for 1 h as positive control. The fluorescence resulting from CellROX® Reagent oxidation was quantified by flow cytometry considering the median fluorescence intensity (MFI) and data shown as fold increase in respect to the average of proliferating samples. For the evaluation of cell debris uptake, target cells were fluorescently labeled with 1.25 µM 5(6)-Carboxyfluorescein diacetate N-succinimidyl ester (CFSE) (Sigma-Aldrich, #21888) and after plating co-cultured with neutrophils at effector:target ratio of 1:2 for 2 h at 37°C. Neutrophils were then collected and analyzed by flow cytometry.

Statistical analysis

All statistical analyses were carried out using GraphPad Prism 8.0.2 (San Diego, CA, USA). For comparisons between two groups, a two-tailed unpaired t-test was used. For multi-group comparison, a one-way or two-way ANOVA with Tukey's post hoc test was performed.

Results

To validate our model of therapy-induced senescence (TIS), we firstly quantified the cytostatic effect of the CDK4/6 inhibitor palbociclib by analyzing the cell cycle of human breast cancer cells following palbociclib treatment. We treated both estrogen-sensitive MCF7 and metastatic triple negative breast cancer MDA-MB-231 cell lines with 2 µM palbociclib for 7 days. Cells were further analyzed after washing out the drug from the culture medium at days 10 (7 days of treatment plus 3 days of recovery) and 14 (7 days of treatment plus 7 days of recovery) to verify the reversibility of the result (Fig. 1A). Palbociclib was able to induce a reversible cell cycle arrest in the G1 phase (Fig. 1B and Supplementary Fig. 1) along with an enlargement of the cell size and increased granularity (Fig. 1C), which reverted after palbociclib removal. To ascribe the transient proliferation arrest to the establishment of a senescence program, we performed the senescence-associated β-galactosidase (SA-β-Gal) assay (Fig. 1D). As additional marker of cellular senescence, we evaluated the loss of perinuclear lamin-B1 by immunofluorescence (Fig. 1E). Besides triggering senescence, palbociclib treatment had little impact on cell death or apoptosis induction as indicated by Annexin V assay

(Fig. 1F). Overall, our results show that palbociclib induces a reversible cell cycle arrest with features of cellular senescence in breast cancer cells, prompting us to further study its immunomodulatory effects.

We focused our attention on the SASP composition, which can widely shape the tumor microenvironment and act on neutrophil recruitment and activation. To this aim, we analyzed the SASP of MCF7 and MDA-MB-231 cells treated with 2 µM palbociclib for 7 days (hereafter named senescent cells) by performing a cytokine screening assay. In particular, we carried out a magnetic bead-based multiplex assay for the Luminex® platform with 24 h-conditioned media (Fig. 2A). The cytokines measured are listed in Table 1. Secretion of CCL2, CXCL10, and IL-1β was increased by senescent MCF7 and MDA-MB-231 cells compared to control proliferating cells (Table 1), confirming the inflammatory feature of a bona fide SASP. IL-6 and IL-8 (CXCL8) are two key factors of the innate immunity affecting neutrophils and frequently upregulated in the SASP, thus they were analyzed separately by ELISA. Both cytokines were largely secreted by senescent MDA-MB-231 cells, while no IL-6 and only a slight increase of IL-8 was observed in senescent MCF7 cell-derived samples (Fig. 2B). These results are in accordance with published data about the inhibitory control of the estrogen receptor over IL-6 and IL-8 expression [48–50]. The presence of IL-8 in the SASP prompted us to investigate whether neutrophils can be effectively recruited by senescent cells. To this aim, we firstly analyzed the expression of CXCL1, CXCL5, CXCL6, CXCL7, and CXCL8, ligands of the chemotactic receptor for neutrophils CXCR2, by quantitative real-time PCR (Fig. 2C). Both cell lines, even if with a different gene profile, showed upregulation of a variety of chemokines, supporting the hypothesis that senescent cells can actively recruit neutrophils. To verify this hypothesis, we evaluated the capacity of conditioned media of attracting neutrophils. Neutrophils were isolated from the blood of healthy donors and assessed in a trans-well migration assay. Neutrophil enrichment, as estimated by CD10, CD15, and CD16 staining, was above 95% and vitality above 95% (Supplementary Fig. 2). A neutralizing anti-IL-8 antibody was used to verify IL-8 specific contribution to migration. Senescent cell-conditioned media enhanced neutrophil migration compared to control proliferating cell-conditioned media. In addition, the migration induced by MDA-MB-231 cell-conditioned medium was partially reverted by IL-8 blocking, in agreement with the high expression of IL-8 measured for this cell line (Fig. 2D). These results demonstrate that tumor cells led to senescence by palbociclib promote neutrophil recruitment.

Besides inflammatory cytokines, the SASP includes damage-associated molecular patterns (DAMPs) [51] that are critical regulators of neutrophil activation. In particular,

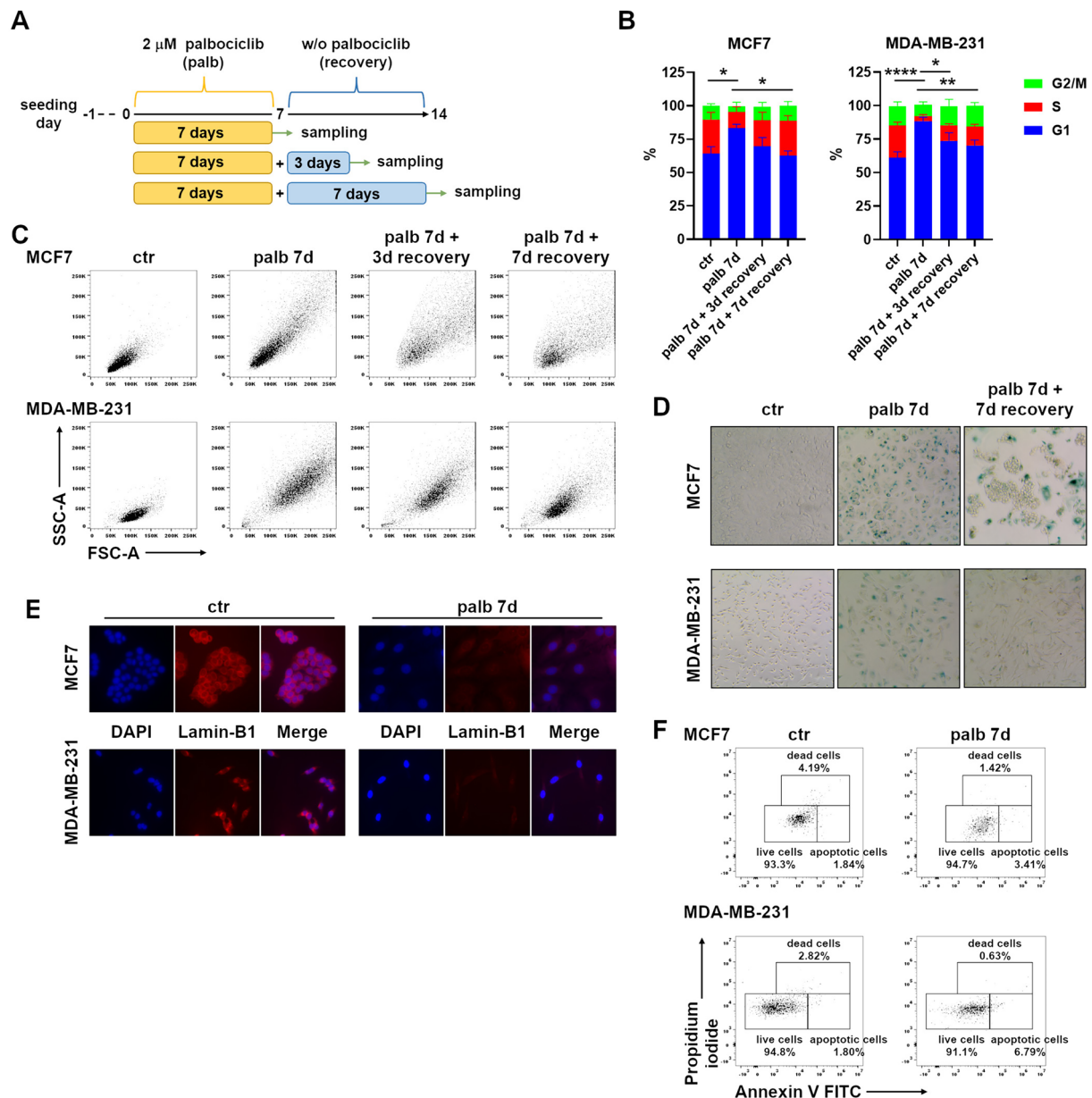


Fig. 1 Palbociclib induces reversible senescence in breast cancer cell lines. **A** Diagram depicting the experimental design. **B** Cell cycle analysis of MCF7 and MDA-MB-231 cells treated with 2 μ M palbociclib as outlined in Fig. 1A. Bars show mean \pm SEM from three independent flow cytometric experiments. Statistical analysis was performed using two-way ANOVA followed by Tukey's multiple-comparisons test. * $P < 0.05$, ** $P < 0.01$, **** $P < 0.0001$ comparing the G1 phase. **C** MCF7 and MDA-MB-231 cell morphology after palbociclib treatment as evaluated by forward and side scatter flow cytometric parameters. **D** Senescence-associated β -galactosidase

(SA- β -Gal) assay of MCF7 and MDA-MB-231 cells after one week of 2 μ M palbociclib and a further week without palbociclib. Blue staining marks senescent cells. Images are representative of more than three independent experiments. Magnification 200 \times . **E** Representative immunofluorescence images of DAPI and Lamin-B1 staining of MCF7 and MDA-MB-231 cells treated with 2 μ M palbociclib for 1 week. Magnification 400 \times . **F** Cell death and apoptosis of MCF7 and MDA-MB-231 cells upon palbociclib treatment as evaluated by Annexin V assay. Representative dot plots of two independent experiments

the acute-phase serum amyloids A1 and A2 (SAAs) have been reported to be key factors of the SASP acting in a paracrine way to reinforce the senescence phenotype [52]. Furthermore, SAA1 synergizes with chemokines in recruiting leukocytes [53]. Thus, we investigated the involvement

of SAA1 as an additional chemoattractant and neutrophil-activating factor. Gene expression of *SAA1* and *SAA2* was significantly increased by senescent cells in both cell lines as evaluated by quantitative real-time PCR (Fig. 3A). We confirmed increased protein production and secretion of

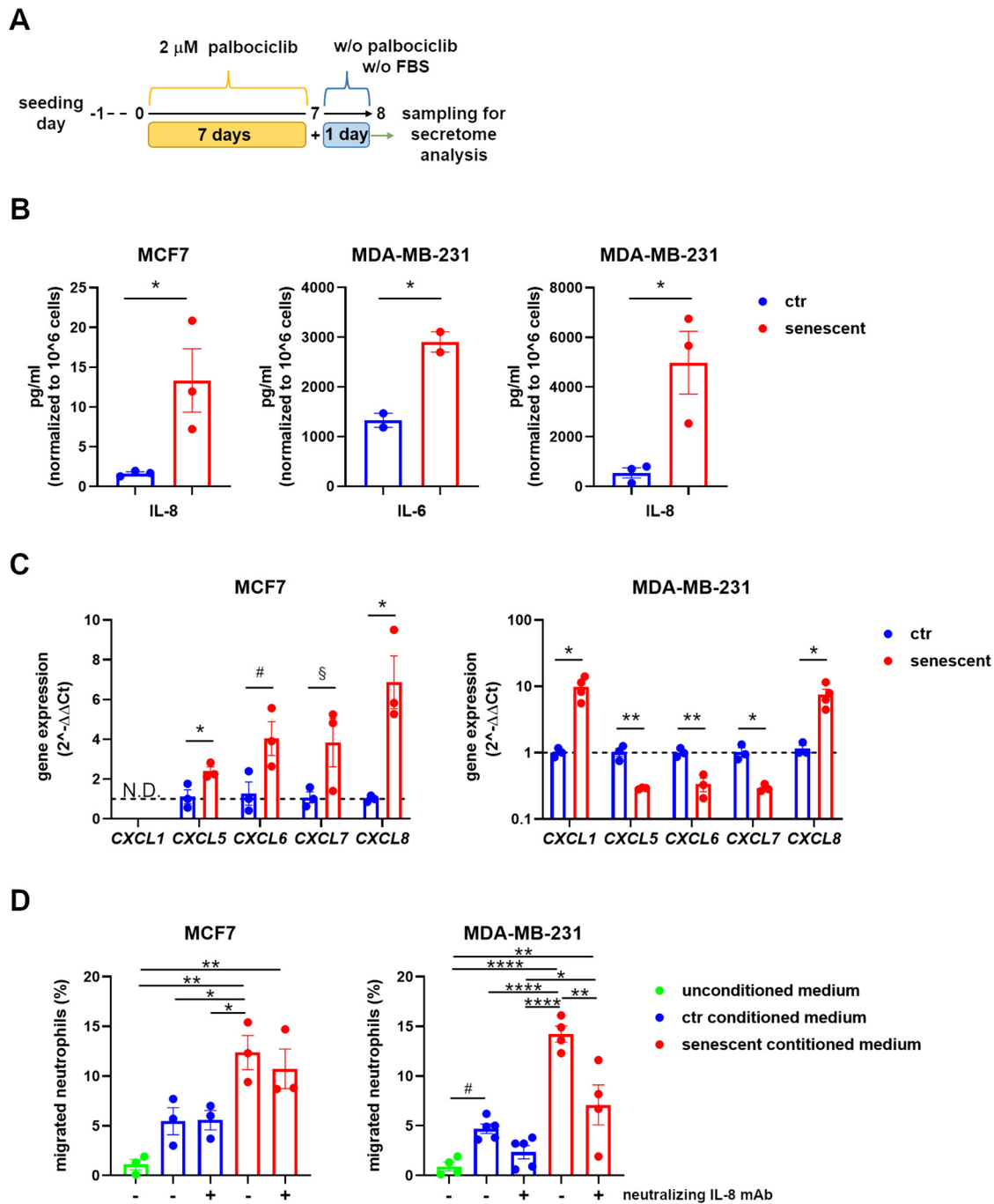


Fig. 2 Senescent MCF7 and MDA-MB-231 cells recruit neutrophils. **A** Diagram depicting the experimental design for conditioned medium analysis. **B** Quantification by ELISA of IL-6 and IL-8 secreted by control proliferating and senescent MCF7 and MDA-MB-231 cells in 24 h-conditioned media as outlined in Fig. 2A. Bars show mean \pm SEM and statistical significance was determined by unpaired two-tailed Student's t-test. * $P < 0.05$. **C** Quantitative real-time PCR of the indicated CXCR2 ligands from total RNA extracted from control proliferating and senescent MCF7 and MDA-MB-231 cells. Data are reported as fold increase by using the $2^{-\Delta\Delta Ct}$ method and the average of control samples for the $\Delta\Delta$ calculation. Bars show mean \pm SEM from at least three independent experiments. Statisti-

cal analysis was performed using multiple t-test (one for each gene of interest). * $P < 0.05$, ** $P < 0.01$, # $P = 0.055$, § $P = 0.092$. N.D. = not detected. **D** Percentage of neutrophils migrated toward conditioned media obtained from control proliferating and senescent MCF7 and MDA-MB-231 cells. Migration toward medium alone (unconditioned medium) was considered as background. Experiments were performed both in the absence and in the presence of neutralizing IL-8 mAb as indicated. Bars show mean \pm SEM from at least three independent experiments. Statistical analysis was performed using one-way ANOVA followed by Tukey's multiple-comparisons test. * $P < 0.05$, ** $P < 0.01$, **** $P < 0.0001$, # $P = 0.087$

Table 1 SASP analysis. Cytokines from conditioned media were quantified by a multi-analyte human magnetic Luminex® assay

Cytokine (pg/ml)	MCF7		MDA-MB-231	
	Ctrl	Senescent	Ctrl	Senescent
CCL2	76.03	315.85	36.50	242.09
CCL27	<LOD	<LOD	<LOD	<LOD
CCL3	<LOD	<LOD	194.65	210.88
CCL4	188.99	205.08	304.92	304.92
CCL7	<LOD	<LOD	<LOD	<LOD
Chemerin	<LOD	<LOD	1241.74	1366.73
CX3CL1	<LOD	<LOD	<LOD	<LOD
CXCL10	4.73	40.64	13.42	34.77
CXCL9	998.77	998.77	1046.58	1046.58
GM-CSF	3.48	6.21	646.85	354.65
IFN- γ	<LOD	<LOD	3.66	5.98
IL-10	2.34	3.62	3.02	3.62
IL-12	<LOD	<LOD	<LOD	<LOD
IL-13	<LOD	<LOD	<LOD	<LOD
IL-15	<LOD	<LOD	<LOD	<LOD
IL-18	14.73	18.41	20.26	22.11
IL-1α	<LOD	<LOD	9.22	40.12
IL-1β	<LOD	1.61	3.25	27.58
IL-2	12.79	20.51	94.85	107.08
IL-21	<LOD	<LOD	<LOD	<LOD
IL-28A	<LOD	<LOD	<LOD	<LOD
IL-4	<LOD	<LOD	43.00	43.00
IL-5	1.14	1.14	4.02	4.02

Cytokines upregulated by senescent cells are highlighted in bold
<LOD indicates values below the limit of detection of the assay

SAA1 by senescent cells analyzing the conditioned media by ELISA (Fig. 3B). These data suggest that neutrophils, once recruited by senescent tumor cells, may be activated by sensing DAMPs in the tumor bed. To extend the relevance of these findings and to verify that senescence per se, independently of palbociclib effects, is responsible for neutrophil engagement, we measured the amount of IL-8 and SAA1 secreted by: (1) proliferating early passage primary fibroblasts; (2) serum-starved early passage primary fibroblasts, in which the cell cycle is temporarily halted (quiescent fibroblasts); (3) late passage primary fibroblasts, which are rendered senescent by replicative exhaustion. To reach replicative senescence human foreskin fibroblasts were subcultured until they progressively acquired an enlarged, flattened morphology and stopped dividing. Cell cycle withdrawal and senescence status were verified by cell cycle analysis and SA- β -Gal assay (Supplementary Fig. 3 and Supplementary Fig. 4). We observed that only senescent fibroblasts increased IL-8 and SAA1 secretion, while quiescent fibroblasts released IL-8 and SAA1 at levels comparable to proliferating fibroblasts (Fig. 3C). These

results indicate that senescent cells, regardless the type of senescence, are endowed with a program intrinsically able to engage neutrophils.

To assess the phenotype of neutrophils after recruitment by senescent cells, we firstly analyzed their morphology by fluorescently tagged phalloidin, as cell shape polarization is considered an early sign of neutrophil activation. Neutrophils exposed to senescent cell-conditioned media exhibited protrusions and loss of circularity, as evaluated by cell edge analysis performed by ImageJ software, while neutrophils incubated with control proliferating cell-conditioned media maintained the rounded appearance typical of resting neutrophils (Fig. 4A and Supplementary Fig. 5). The capacity of NET extrusion is a peculiar feature of activated neutrophils also in sterile inflammation. Thus, we evaluated the release of nuclear material in the form of NETs by staining neutrophils cultured with proliferating cell- or senescent cell-conditioned media with a dye labeling extracellular DNA (SYTOX Green). Strikingly, NET formation was only observed in the presence of conditioned media derived from senescent cells (Fig. 4B). NET generation is often coupled with ROS production; for this reason, we quantified ROS by using cell-permeable fluorogenic probes designed to measure ROS in live cells (CellROX® Oxidative Stress Reagents). A slight increase of ROS was detected by flow cytometry in neutrophils incubated with senescent cell-conditioned media compared to neutrophils incubated with control proliferating cell-conditioned media (Fig. 4C). Finally, to investigate a possible role of activated neutrophils in tissue remodeling, we addressed their clearance capacity of senescent tumor cells by co-culture. Neutrophils were seeded upon fluorescently CFSE-labeled proliferating or senescent MCF7 and MDA-MB-231 cells and the acquisition of the CFSE fluorescence, suggestive of cell debris uptake, was evaluated by flow cytometry. Neutrophils performed better uptake of senescent cell debris than debris of control proliferating cells (Fig. 4D and Supplementary Fig. 6), suggesting that senescent cells have increased susceptibility to neutrophil-mediated clearance. Overall, these results demonstrate that palbociclib-induced senescence, even in the absence of a permanent cell cycle arrest, is characterized by an inflammatory secretome that drives neutrophil recruitment and activation, likely triggering a local immune reaction and tissue remodeling (Fig. 5).

Discussion

Cellular senescence has been recently proposed as an emerging hallmark of cancer [54]. However, the impact of senescent cells on tumor immune microenvironment remains incompletely understood [55]. Senescent tumor cells contribute to adjuvanticity and antigenicity but also trigger

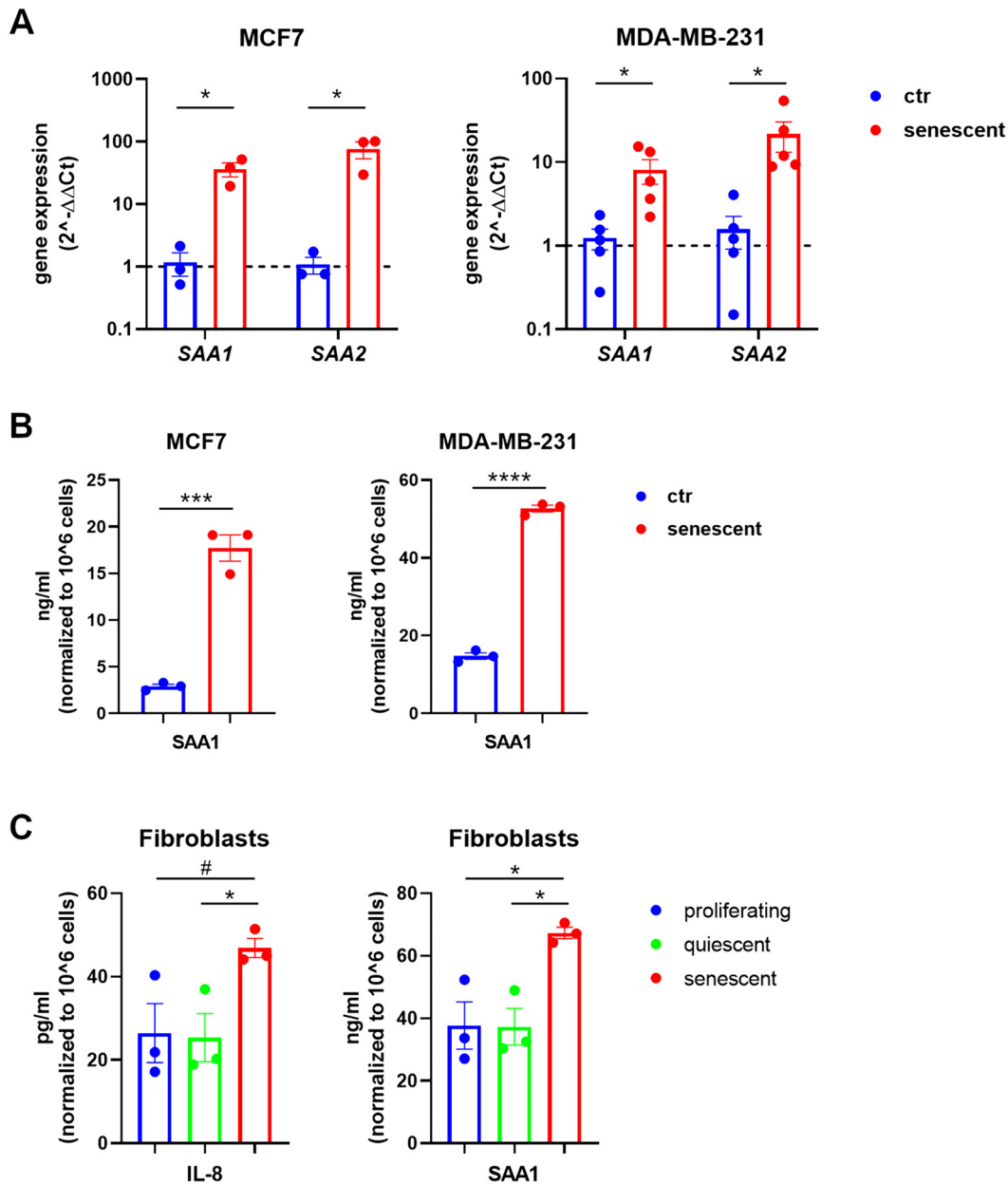
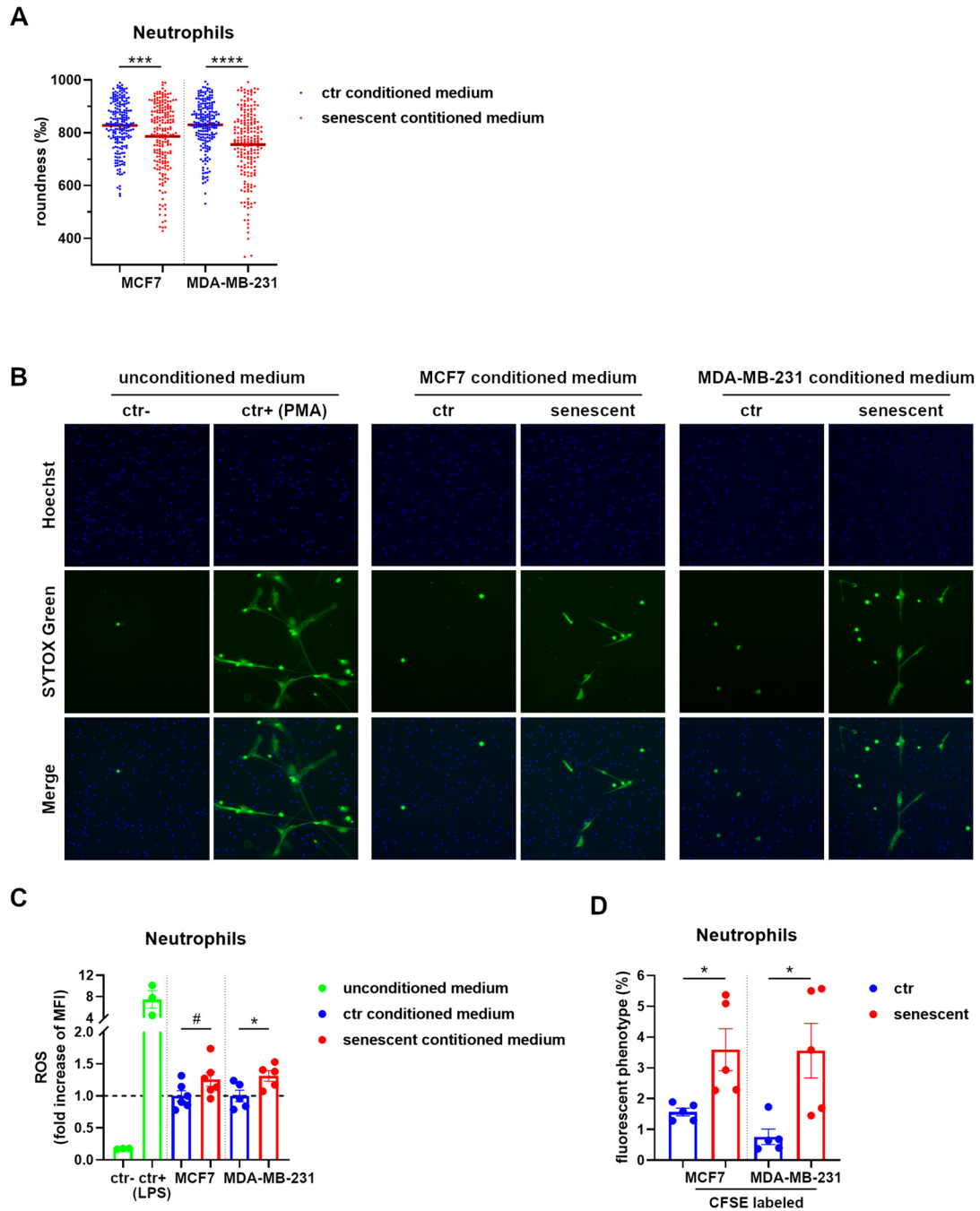


Fig. 3 Senescent cells express recruiting and activating factors for neutrophils. **A** Quantitative real-time PCR of *SAA1* and *SAA2* genes from total RNA extracted from control proliferating and senescent MCF7 and MDA-MB-231 cells. Data are reported as fold increase by using the $2^{-\Delta\Delta Ct}$ method and the average of control samples for the $\Delta\Delta$ calculation. Bars show mean \pm SEM from at least three independent experiments. Statistical analysis was performed using multiple t-test (one for each gene of interest). * $P < 0.05$. **B** Quantification by ELISA of SAA1 secreted by control proliferating and senescent

MCF7 and MDA-MB-231 cells in 24 h-conditioned media. Bars show mean \pm SEM and statistical significance was determined by unpaired two-tailed Student's t-test. *** $P < 0.001$, **** $P < 0.0001$. **C** Quantification by ELISA of IL-8 and SAA1 secreted by proliferating, quiescent, and senescent human foreskin fibroblasts in 24 h-conditioned media. Bars show mean \pm SEM and statistical significance was determined by one-way ANOVA followed by Tukey's multiple-comparisons test. * $P < 0.05$, # $P = 0.091$

immune checkpoint expression, heterogeneously affecting innate and adaptive immunity [56, 57]. In our study, we aimed to explore the potential role of neutrophils in this context, addressing their recruitment and activation by

senescent tumor cells. Given the clinical relevance of TIS in cancer treatment, we focused our study on the CDK4/6 inhibitor palbociclib, which is approved for the treatment of breast cancer and is under intense investigation for



additional malignancies. In the present study, we showed that: (1) palbociclib makes tumor cells senescent with a reversible phenotype; (2) the senescent phenotype induced by palbociclib is endowed with an inflammatory secretome that can recruit and activate neutrophils through the release of different inflammatory factors, such as IL-8 and SAA1; (3) the activated neutrophils are able to perform phagocytic removal of senescent tumor cells. These findings have different implications. The reversibility of the palbociclib-induced senescence should be considered therapeutically relevant

as the current clinical schedule for palbociclib is based on three weeks of administration followed by one week of stop. Long-term effects of CDK4/6 inhibition strictly depend on the duration of the treatment or genetic background (i.e., p53 status) of cancer cells as recently suggested [58, 59]. Transient cell cycle arrest may be due to an incomplete senescence program as senescence is a biological continuum and highly dynamic process rather than a terminally defined condition. Different states may exist, ranging from “light” to “deep” senescence, likely differing in some aspects. A global

Fig. 4 Secretome of senescent MCF7 and MDA-MB-231 cells promotes neutrophil activation. **A** Circularity score of neutrophils stimulated with the conditioned media obtained from control proliferating and senescent MCF7 and MDA-MB-231 cells. Cell shape was visualized by phalloidin staining and roundness calculated with the ImageJ software. Each dot represents the corresponding value (1000 indicates precise round shape) of a single cell. The horizontal red bar represents the mean value. Statistical analysis was performed using unpaired two-tailed Student's t-test (one for each cell line). *** $P < 0.001$, **** $P < 0.0001$. **B** NET formation by neutrophils stimulated with the conditioned media obtained from control proliferating and senescent MCF7 and MDA-MB-231 cells. Medium alone (with FBS) and medium with PMA were used as negative and positive control, respectively. Nuclei and NETs were visualized by Hoechst and SYTOX Green staining, respectively. Images are representative of two independent experiments. Magnification 100 \times . **C** ROS production by neutrophils stimulated with the conditioned media obtained from control proliferating and senescent MCF7 and MDA-MB-231 cells. Medium alone (with FBS) and medium with LPS were used as negative and positive control, respectively. ROS were quantified by flow cytometry considering the median fluorescence intensity (MFI) of ROS-specific fluorogenic probes. Data are reported as fold increase in respect to the average of corresponding control proliferating samples. Bars show mean \pm SEM from at least three independent experiments. Statistical analysis was performed using unpaired two-tailed Student's t-test (one for each cell line). * $P < 0.05$, # $P = 0.088$. **D** Evaluation of the uptake by neutrophils of CFSE-labeled control proliferating or senescent MCF7 and MDA-MB-231 cells as evaluated by flow cytometry. Graphs show the percentage of neutrophils acquiring the CFSE⁺ phenotype. Bars show mean \pm SEM from at least three independent experiments. Statistical analysis was performed using unpaired two-tailed Student's t-test (one for each cell line). * $P < 0.05$

epigenetic reprogramming occurs during time leading to the acquisition of novel cell functions that may still revert totally or only in part [60–62]. Tumor regrowth and/or acquisition of stemness features by senescent tumor cells after cell cycle reentry have been described and must be avoided [63]. In addition, a speculative idea is now linking senescence to cancer dormancy, with yet unexplored implications [64]. It is interesting to notice that sustained activity of the mTOR pathway has been linked to the acquisition of the senescent phenotype [65, 66]. Thus, modulating the activity of the mTORC1 and mTORC2 complexes, in principle, might be exploited to avoid senescence entry or, on the contrary, to force cells into a permanent state of senescence. Alternative strategies can rely on the direct targeting of senescent cells. Indeed, senescent cells can be specifically targeted by senolytics and senomorphics, agents aimed at selectively eliminating senescent cells and abrogating/modulating the SASP, respectively [67, 68]. Steps into this direction are moving fast, and trials with senotherapeutic compounds, especially for age-related diseases, are ongoing [69]. Combined therapies implementing palbociclib with mTOR-targeting drugs or senotherapeutics could significantly improve treatments efficacy and could be accompanied by dosage lowering, with the aim of reducing side effects.

Regarding the SASP-evoked immune response, the neutrophil engagement by senescent tumor cells adds further

complexity to the immune scenario. Neutrophil recruitment can be beneficial by promoting direct antitumor response in preneoplastic lesions or by switching “cold” tumors into “hot” ones. However, it may also be detrimental in the event of unresolved inflammation. In this regard, we demonstrated that activation of neutrophils upon stimulation with senescent cell secretome results in NET formation. In the context of tumors, NETosis is mostly associated with an unfavorable tumor microenvironment due to tissue damage and release of proinflammatory factors that lead to epithelial to mesenchymal transition (EMT) and angiogenesis, paving the way to metastatic processes [70]. In breast cancer, NETosis has been associated with disease worsening and vasculature adverse events [71]. Myeloperoxidase (MPO) participates in NET release by moving from the cytosol to the nucleus where it contributes to nuclear membrane breakdown. MPO is then entrapped in the extruded materials and drives the production of anti-neutrophil cytoplasmic antibodies (ANCA), which have been reported to play a role in the pathogenesis of autoimmune diseases [72]. However, to which extent ANCA or the exposure of DAMPs by NETs shape tumor immunity is largely unknown. On the one hand, ANCA have been reported in cancer patients with vasculitis [73], thus serving as potent inflammatory factors, on the other hand, NETosis may provide adjuvant factors eliciting tumor neoantigen-driven responses. Recently, it has been shown that NETs can act as scaffold for the release of factors with antitumoral activity, i.e., cathepsin G, or, in the opposite direction, promoting EMT in cancer cells, i.e., TGF- β [74, 75].

Our secretome analysis uncovered SAA1 as a major factor of the SASP of palbociclib-induced senescent tumor cells. This acute-phase protein is a serum factor whose precise biological functions are still unresolved [53, 76, 77]. Interestingly, SAA1 (primarily through its derived peptides) appears to have differing impact on neutrophil phenotype, enhancing the inflammatory response when neutrophils reach the site of injury, but pushing toward a pro-resolving function during the resolution stage of inflammation [78]. It is tempting to speculate that senescent cells, partially by modulating SAA1, orchestrate inflammation and its resolution through a coordinate program that includes neutrophil switching from an “N1” to an “N2” phenotype. From an evolutionary perspective, cellular senescence is reasonably related to tissue healing rather than tumor suppressive mechanism [79, 80]. Following tissue injury, the induction of senescence prevents the spreading of the insult by arresting the proliferation of damaged cells and then elicits tissue remodeling by providing a plethora of bioactive factors in the microenvironment. This perspective explains the ability of senescent cells to recruit the immune system to trigger their clearance and, at the same time, to promote stemness

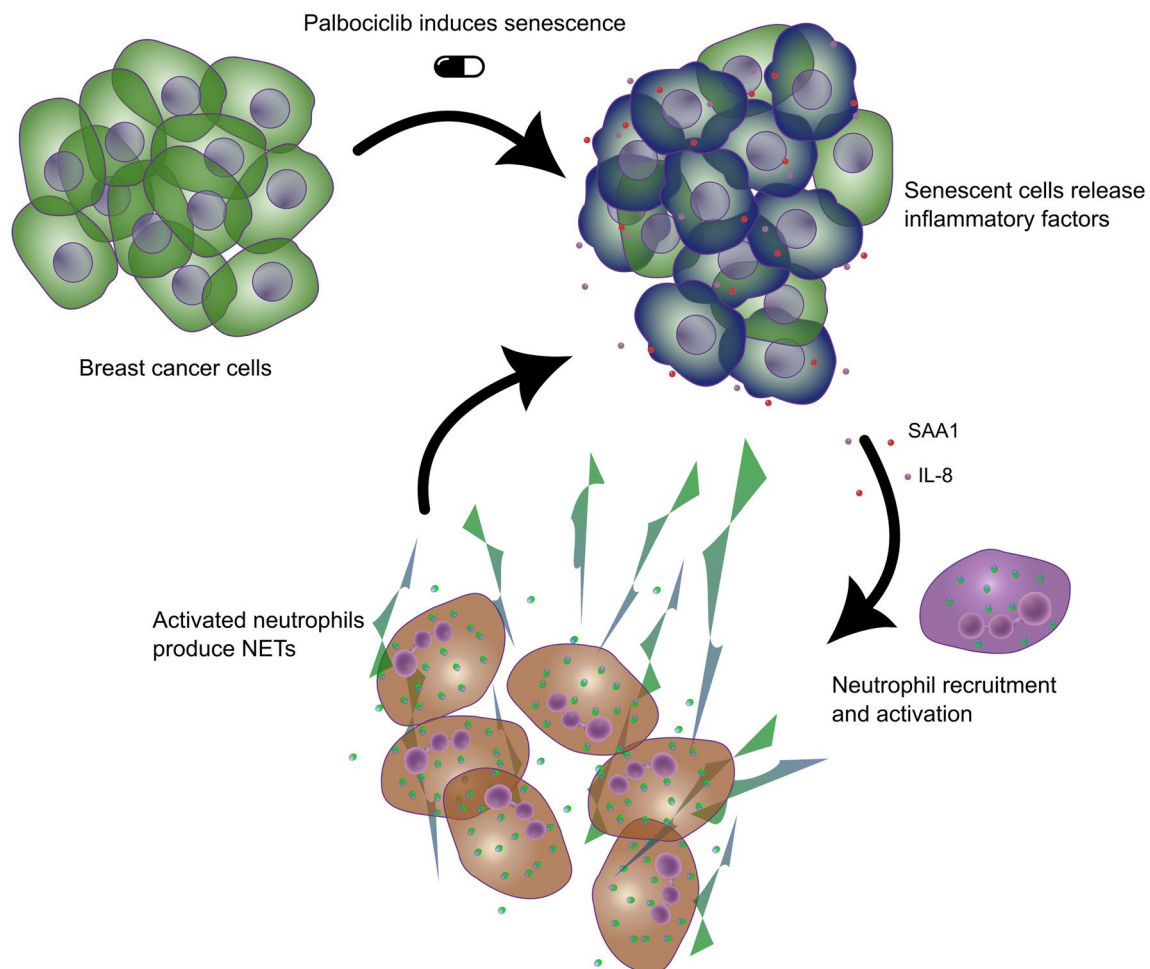


Fig. 5 Senescence by palbociclib recruits and activates neutrophils. Breast cancer cells induced to senescence by the CDK4/6 inhibitor palbociclib release IL-8 and SAA1, which, in turn, recruit and activate neutrophils causing NET production in tumor

features in the surrounding cells to enhance tissue repair. Unwantedly, this mechanism is exploited by cancer cells, favoring tumor progression. Therefore, there is an urgent need to separate tumor-inhibiting from tumor-promoting effects of senescence. IL-8 is a key chemokine involved in cancer plasticity and immune suppression [81]. In our study, we reported its upregulation by senescent cells and its effect on neutrophils. Interestingly, levels of IL-8, as well as levels of IL-6 and SSA1, were reminiscent of the baseline expression in not-senescent parental cells, supporting the finding that SASP factors are strictly related to original cell type, likely due to chromatin background, as already postulated [82]. Given that the IL-8/IL-8R axis is already a therapeutic target in different clinical studies [81], this approach could be considered to mitigate the side effects of senescence. It is now emerging that senescent cells play a prominent role during aging and aging-related disorders, including cancer, thus it is of great relevance depicting the entire immune

landscape induced by cellular senescence to better tailor the upcoming therapies.

Supplementary Information The online version contains supplementary material available at <https://doi.org/10.1007/s00262-024-03695-5>.

Acknowledgements The authors gratefully thank Dr. Francesca Di Rosa (National Research Council of Italy) for helpful discussion.

Author contributions ASa, and FA conceived the study; GF, MNR, and FA designed experiments; GF, MNR, LC, ML, and FA performed and analyzed experiments; MC, ASo, SS, and ASa contributed intellectually and provided technical support; FA wrote the manuscript with input from all authors; GF, MNR, LC, ML, MC, ASo, SS, ASa, and FA approved the final version of the article.

Funding Open access funding provided by Consiglio Nazionale Delle Ricerche (CNR) within the CRUI-CARE Agreement. This work was supported by an Investigator-Initiated Research (IIR) Program WI240713 from Pfizer Inc. to ASa; Progetto di Ricerca 2019 RP11916B79E083FC from Sapienza University of Rome to FA; project DBA.AD005.225—NUTRAGE—FOE2021 from Consiglio Nazionale delle Ricerche (CNR); Progetto di Ricerca 2020 RM120172A77458FC

from Sapienza University of Rome to ASO; European Union—Next Generation EU, in the context of The National Recovery and Resilience Plan, Investment Partenariato Esteso PE8 “Conseguenze e sfide dell’invecchiamento,” Project Age-It (Ageing Well in an Ageing Society) to SS, and the same grant sustained ML fixed-term researcher position; National Funding for Centers of Excellence (Science Department 2023–2027, Roma Tre University, MIUR, Articolo 1, Commi 314–337, Legge 232/2016).

Data availability The data that support the findings of this study are available from the corresponding author upon reasonable request.

Declarations

Conflict of interest The authors have no conflicts of interest to declare that are relevant to the content of this article.

Open Access This article is licensed under a Creative Commons Attribution 4.0 International License, which permits use, sharing, adaptation, distribution and reproduction in any medium or format, as long as you give appropriate credit to the original author(s) and the source, provide a link to the Creative Commons licence, and indicate if changes were made. The images or other third party material in this article are included in the article's Creative Commons licence, unless indicated otherwise in a credit line to the material. If material is not included in the article's Creative Commons licence and your intended use is not permitted by statutory regulation or exceeds the permitted use, you will need to obtain permission directly from the copyright holder. To view a copy of this licence, visit <http://creativecommons.org/licenses/by/4.0/>.

References

- Galluzzi L, Vitale I, Aaronson SA et al (2018) Molecular mechanisms of cell death: recommendations of the Nomenclature Committee on cell death 2018. *Cell Death Differ* 25:486–541. <https://doi.org/10.1038/s41418-017-0012-4>
- Gluck S, Guey B, Gulen MF et al (2017) Innate immune sensing of cytosolic chromatin fragments through cGAS promotes senescence. *Nat Cell Biol* 19:1061–1070. <https://doi.org/10.1038/ncb3586>
- Gorgoulis V, Adams PD, Alimonti A et al (2019) Cellular senescence: defining a path forward. *Cell* 179:813–827. <https://doi.org/10.1016/j.cell.2019.10.005>
- Ou HL, Hoffmann R, Gonzalez-Lopez C, Doherty GJ, Korkola JE, Munoz-Espin D (2021) Cellular senescence in cancer: from mechanisms to detection. *Mol Oncol* 15:2634–2671. <https://doi.org/10.1002/1878-0261.12807>
- Chibaya L, Snyder J, Ruscetti M (2022) Senescence and the tumor-immune landscape: Implications for cancer immunotherapy. *Semin Cancer Biol* 86:827–845. <https://doi.org/10.1016/j.semcancer.2022.02.005>
- Di Mitri D, Alimonti A (2016) Non-cell-autonomous regulation of cellular senescence in cancer. *Trends Cell Biol* 26:215–226. <https://doi.org/10.1016/j.tcb.2015.10.005>
- Kumari R, Jat P (2021) Mechanisms of cellular senescence: cell cycle arrest and senescence associated secretory phenotype. *Front Cell Dev Biol* 9:645593. <https://doi.org/10.3389/fcell.2021.645593>
- Schmitt CA, Wang B, Demaria M (2022) Senescence and cancer - role and therapeutic opportunities. *Nat Rev Clin Oncol* 19:619–636. <https://doi.org/10.1038/s41571-022-00668-4>
- Iannello A, Thompson TW, Ardolino M, Lowe SW, Raulet DH (2013) p53-dependent chemokine production by senescent tumor cells supports NKG2D-dependent tumor elimination by natural killer cells. *J Exp Med* 210:2057–2069. <https://doi.org/10.1084/jem.20130783>
- Ruscetti M, Leibold J, Bott MJ et al (2018) NK cell-mediated cytotoxicity contributes to tumor control by a cytostatic drug combination. *Science* 362:1416–1422. <https://doi.org/10.1126/science.aas9090>
- Xue W, Zender L, Miething C, Dickins RA, Hernando E, Krizhanovsky V, Cordon-Cardo C, Lowe SW (2007) Senescence and tumour clearance is triggered by p53 restoration in murine liver carcinomas. *Nature* 445:656–660. <https://doi.org/10.1038/nature05529>
- Antonangeli F, Soriani A, Ricci B, Ponzetta A, Benigni G, Morrone S, Bernardini G, Santoni A (2016) Natural killer cell recognition of in vivo drug-induced senescent multiple myeloma cells. *Oncoimmunology* 5:e1218105. <https://doi.org/10.1080/2162402X.2016.1218105>
- Antonangeli F, Zingoni A, Soriani A, Santoni A (2019) Senescent cells: living or dying is a matter of NK cells. *J Leukoc Biol* 105:1275–1283. <https://doi.org/10.1002/JLB.MR0718-299R>
- Sagiv A, Biran A, Yon M, Simon J, Lowe SW, Krizhanovsky V (2013) Granule exocytosis mediates immune surveillance of senescent cells. *Oncogene* 32:1971–1977. <https://doi.org/10.1038/onc.2012.206>
- Sagiv A, Burton DG, Moshayev Z, Vadai E, Wensveen F, Ben-Dor S, Golani O, Polic B, Krizhanovsky V (2016) NKG2D ligands mediate immunosurveillance of senescent cells. *Aging (Albany NY)* 8:328–344. <https://doi.org/10.18632/aging.100897>
- Soriani A, Zingoni A, Cerboni C et al (2009) ATM-ATR-dependent up-regulation of DNAM-1 and NKG2D ligands on multiple myeloma cells by therapeutic agents results in enhanced NK-cell susceptibility and is associated with a senescent phenotype. *Blood* 113:3503–3511. <https://doi.org/10.1182/blood-2008-08-173914>
- Kale A, Sharma A, Stolzing A, Desprez PY, Campisi J (2020) Role of immune cells in the removal of deleterious senescent cells. *Immun Ageing* 17:16. <https://doi.org/10.1186/s12979-020-00187-9>
- Kang TW, Yevsa T, Woller N et al (2011) Senescence surveillance of pre-malignant hepatocytes limits liver cancer development. *Nature* 479:547–551. <https://doi.org/10.1038/nature10599>
- Chen HA, Ho YJ, Mezzadra R et al (2023) Senescence rewires microenvironment sensing to facilitate antitumor immunity. *Cancer Discov* 13:432–453. <https://doi.org/10.1158/2159-8290.CD-22-0528>
- Marin I, Boix O, Garcia-Garijo A et al (2023) Cellular senescence is immunogenic and promotes antitumor immunity. *Cancer Discov* 13:410–431. <https://doi.org/10.1158/2159-8290.Cd-22-0523>
- Ruhland MK, Alspach E (2021) Senescence and immunoregulation in the tumor microenvironment. *Front Cell Dev Biol* 9:754069. <https://doi.org/10.3389/fcell.2021.754069>
- Milanovic M, Fan DNY, Belenki D et al (2018) Senescence-associated reprogramming promotes cancer stemness. *Nature* 553:96–100. <https://doi.org/10.1038/nature25167>
- Pereira BI, Devine OP, Vukmanovic-Stejic M et al (2019) Senescent cells evade immune clearance via HLA-E-mediated NK and CD8(+) T cell inhibition. *Nat Commun* 10:2387. <https://doi.org/10.1038/s41467-019-10335-5>
- Ruhland MK, Loza AJ, Capietto AH et al (2016) Stromal senescence establishes an immunosuppressive microenvironment that drives tumorigenesis. *Nat Commun* 7:11762. <https://doi.org/10.1038/ncomms11762>
- Binet F, Cagnone G, Crespo-Garcia S et al (2020) Neutrophil extracellular traps target senescent vasculature for tissue remodeling in retinopathy. *Science* 369(6506):eaay5356. <https://doi.org/10.1126/science.aay5356>

26. Sen B, Aggarwal S, Nath R et al (2022) Secretome of senescent hepatoma cells modulate immune cell fate by macrophage polarization and neutrophil extracellular traps formation. *Med Oncol* 39:134. <https://doi.org/10.1007/s12032-022-01732-w>
27. Jaillon S, Ponzetta A, Di Mitri D, Santoni A, Bonocchi R, Mantovani A (2020) Neutrophil diversity and plasticity in tumour progression and therapy. *Nat Rev Cancer* 20:485–503. <https://doi.org/10.1038/s41568-020-0281-y>
28. Chen DS, Mellman I (2013) Oncology meets immunology: the cancer-immunity cycle. *Immunity* 39:1–10. <https://doi.org/10.1016/j.immuni.2013.07.012>
29. Galluzzi L, Humeau J, Buque A, Zitvogel L, Kroemer G (2020) Immunostimulation with chemotherapy in the era of immune checkpoint inhibitors. *Nat Rev Clin Oncol* 17:725–741. <https://doi.org/10.1038/s41571-020-0413-z>
30. Sieben CJ, Sturmlechner I, van de Sluis B, van Deursen JM (2018) Two-step senescence-focused cancer therapies. *Trends Cell Biol* 28:723–737. <https://doi.org/10.1016/j.tcb.2018.04.006>
31. Bonelli M, La Monica S, Fumarola C, Alfieri R (2019) Multiple effects of CDK4/6 inhibition in cancer: from cell cycle arrest to immunomodulation. *Biochem Pharmacol* 170:113676. <https://doi.org/10.1016/j.bcp.2019.113676>
32. Hendrychova D, Jorda R, Krystof V (2021) How selective are clinical CDK4/6 inhibitors? *Med Res Rev* 41:1578–1598. <https://doi.org/10.1002/med.21769>
33. Petroni G, Formenti SC, Chen-Kiang S, Galluzzi L (2020) Immunomodulation by anticancer cell cycle inhibitors. *Nat Rev Immunol* 20:669–679. <https://doi.org/10.1038/s41577-020-0300-y>
34. Llanos S, Megias D, Blanco-Aparicio C, Hernandez-Encinas E, Rovira M, Pietrocola F, Serrano M (2019) Lysosomal trapping of palbociclib and its functional implications. *Oncogene* 38:3886–3902. <https://doi.org/10.1038/s41388-019-0695-8>
35. Munoz-Espin D, Rovira M, Galiana I et al (2018) A versatile drug delivery system targeting senescent cells. *EMBO Mol Med* 10(9):e9355. <https://doi.org/10.15252/emmm.201809355>
36. Vijayaraghavan S, Karakas C, Doostan I et al (2017) CDK4/6 and autophagy inhibitors synergistically induce senescence in Rb positive cytoplasmic cyclin E negative cancers. *Nat Commun* 8:15916. <https://doi.org/10.1038/ncomms15916>
37. Yoshida A, Lee EK, Diehl JA (2016) Induction of therapeutic senescence in vemurafenib-resistant melanoma by extended inhibition of CDK4/6. *Cancer Res* 76:2990–3002. <https://doi.org/10.1158/0008-5472.CAN-15-2931>
38. Du Q, Guo X, Wang M, Li Y, Sun X, Li Q (2020) The application and prospect of CDK4/6 inhibitors in malignant solid tumors. *J Hematol Oncol* 13:41. <https://doi.org/10.1186/s13045-020-00880-8>
39. Ettl T, Schulz D, Bauer RJ (2022) The renaissance of cyclin dependent kinase inhibitors. *Cancers (Basel)*. 14(2):293. <https://doi.org/10.3390/cancers14020293>
40. Riess C, Irmscher N, Salewski I, Struder D, Classen CF, Grosse-Thie C, Junghans C, Maletzki C (2021) Cyclin-dependent kinase inhibitors in head and neck cancer and glioblastoma-backbone or add-on in immune-oncology? *Cancer Metastasis Rev* 40:153–171. <https://doi.org/10.1007/s10555-020-09940-4>
41. Chen W, Zhang W, Chen M, Yang C, Fang T, Wang H, Reid LM, He Z (2022) Applications and mechanisms of the cyclin-dependent kinase 4/6 inhibitor, PD-0332991, in solid tumors. *Cell Oncol (Dordr)* 45:1053–1071. <https://doi.org/10.1007/s13402-022-00714-4>
42. Klein ME, Kovatcheva M, Davis LE, Tap WD, Koff A (2018) CDK4/6 inhibitors: the mechanism of action may not be as simple as once thought. *Cancer Cell* 34:9–20. <https://doi.org/10.1016/j.ccell.2018.03.023>
43. Birnhuber A, Egemnazarov B, Biasin V, Bonyadi Rad E, Wygrecka M, Olschewski H, Kwapiszewska G, Marsh LM (2020) CDK4/6 inhibition enhances pulmonary inflammatory infiltration in bleomycin-induced lung fibrosis. *Respir Res* 21:167. <https://doi.org/10.1186/s12931-020-01433-w>
44. FDA (2019) U.S. Food and Drug Administration. FDA warns about rare but severe lung inflammation with Ibrance, Kisqali, and Verzenio for breast cancer: FDA Drug Safety Communication.
45. Jost T, Heinzerling L, Fietkau R, Hecht M, Distel LV (2021) Palbociclib induces senescence in melanoma and breast cancer cells and leads to additive growth arrest in combination with irradiation. *Front Oncol* 11:740002. <https://doi.org/10.3389/fonc.2021.740002>
46. Tamura K, Mukai H, Naito Y et al (2016) Phase I study of palbociclib, a cyclin-dependent kinase 4/6 inhibitor, in Japanese patients. *Cancer Sci* 107:755–763. <https://doi.org/10.1111/cas.12932>
47. Cui C, Schoenfelt KQ, Becker KM, Becker L (2021) Isolation of polymorphonuclear neutrophils and monocytes from a single sample of human peripheral blood. *STAR Protoc* 2:100845. <https://doi.org/10.1016/j.xpro.2021.100845>
48. Freund A, Chauveau C, Brouillet JP, Lucas A, Lacroix M, Licznar A, Vignon F, Lazennec G (2003) IL-8 expression and its possible relationship with estrogen-receptor-negative status of breast cancer cells. *Oncogene* 22:256–265. <https://doi.org/10.1038/sj.onc.1206113>
49. Freund A, Jolivel V, Durand S, Kersual N, Chalbos D, Chavey C, Vignon F, Lazennec G (2004) Mechanisms underlying differential expression of interleukin-8 in breast cancer cells. *Oncogene* 23:6105–6114. <https://doi.org/10.1038/sj.onc.1207815>
50. Thirkettle S, Decock J, Arnold H, Pennington CJ, Jaworski DM, Edwards DR (2013) Matrix metalloproteinase 8 (collagenase 2) induces the expression of interleukins 6 and 8 in breast cancer cells. *J Biol Chem* 288:16282–16294. <https://doi.org/10.1074/jbc.M113.464230>
51. Lopes-Paciencia S, Saint-Germain E, Rowell MC, Ruiz AF, Kalegari P, Ferbeyre G (2019) The senescence-associated secretory phenotype and its regulation. *Cytokine* 117:15–22. <https://doi.org/10.1016/j.cyto.2019.01.013>
52. Hari P, Millar FR, Tarrats N et al (2019) The innate immune sensor Toll-like receptor 2 controls the senescence-associated secretory phenotype. *Sci Adv* 5:eaaw0254. <https://doi.org/10.1126/sciadv.aaw0254>
53. Abouelasrar Salama S, De Bondt M, De Buck M et al (2020) Serum amyloid A1 (SAA1) revisited: restricted leukocyte-activating properties of homogeneous SAA1. *Front Immunol* 11:843. <https://doi.org/10.3389/fimmu.2020.00843>
54. Hanahan D (2022) Hallmarks of cancer: new dimensions. *Cancer Discov* 12:31–46. <https://doi.org/10.1158/2159-8290.CD-21-1059>
55. Takasugi M, Yoshida Y, Hara E, Ohtani N (2023) The role of cellular senescence and SASP in tumour microenvironment. *FEBS J* 290:1348–1361. <https://doi.org/10.1111/febs.16381>
56. Hanna A, Balko JM (2023) No rest for the wicked: Tumor cell senescence reshapes the immune microenvironment. *Cancer Cell* 41:831–833. <https://doi.org/10.1016/j.ccell.2023.03.013>
57. Marin I, Serrano M, Pietrocola F (2023) Recent insights into the crosstalk between senescent cells and CD8 T lymphocytes. *NPJ Aging* 9:8. <https://doi.org/10.1038/s41514-023-00105-5>
58. Crozier L, Foy R, Mouery BL, Whitaker RH, Corno A, Spanos C, Ly T, Gowen Cook J, Saurin AT (2022) CDK4/6 inhibitors induce replication stress to cause long-term cell cycle withdrawal. *EMBO J* 41:e108599. <https://doi.org/10.15252/embj.2021108599>
59. Wang B, Varela-Eirin M, Brandenburg SM et al (2022) Pharmacological CDK4/6 inhibition reveals a p53-dependent senescence state with restricted toxicity. *EMBO J* 41:e108946. <https://doi.org/10.15252/embj.2021108946>

60. Lee S, Schmitt CA (2019) The dynamic nature of senescence in cancer. *Nat Cell Biol* 21:94–101. <https://doi.org/10.1038/s41556-018-0249-2>
61. Martinez-Zamudio RI, Roux PF, de Freitas J et al (2020) AP-1 imprints a reversible transcriptional programme of senescent cells. *Nat Cell Biol* 22:842–855. <https://doi.org/10.1038/s41556-020-0529-5>
62. Martinez-Zamudio RI, Stefa A, Nabuco Leva Ferreira Freitas JA et al (2023) Escape from oncogene-induced senescence is controlled by POU2F2 and memorized by chromatin scars. *Cell Genom* 3:100293. <https://doi.org/10.1016/j.xgen.2023.100293>
63. Saleh T, Carpenter VJ, Bloukh S, Gewirtz DA (2022) Targeting tumor cell senescence and polyploidy as potential therapeutic strategies. *Semin Cancer Biol* 81:37–47. <https://doi.org/10.1016/j.semcancer.2020.12.010>
64. DeLuca VJ, Saleh T (2023) Insights into the role of senescence in tumor dormancy: mechanisms and applications. *Cancer Metastasis Rev* 42:19–35. <https://doi.org/10.1007/s10555-023-10082-6>
65. Maskey RS, Wang F, Lehman E et al (2021) Sustained mTORC1 activity during palbociclib-induced growth arrest triggers senescence in ER+ breast cancer cells. *Cell Cycle* 20:65–80. <https://doi.org/10.1080/15384101.2020.1859195>
66. Walters HE, Deneka-Hannemann S, Cox LS (2016) Reversal of phenotypes of cellular senescence by pan-mTOR inhibition. *Aging (Albany NY)* 8:231–244. <https://doi.org/10.18632/aging.100872>
67. Cuollo L, Antonangeli F, Santoni A, Soriani A (2020) The senescence-associated secretory phenotype (sasp) in the challenging future of cancer therapy and age-related diseases. *Biology (Basel)* 9:485. <https://doi.org/10.3390/biology9120485>
68. Ovadya Y, Krizhanovsky V (2018) Strategies targeting cellular senescence. *J Clin Invest* 128:1247–1254. <https://doi.org/10.1172/JCI95149>
69. Borghesan M, Hoogaars WMH, Varela-Eirin M, Talma N, Demaria M (2020) A senescence-centric view of aging: implications for longevity and disease. *Trends Cell Biol* 30:777–791. <https://doi.org/10.1016/j.tcb.2020.07.002>
70. Jaboury S, Wang K, O'Sullivan KM, Ooi JD, Ho GY (2023) NETosis as an oncologic therapeutic target: a mini review. *Front Immunol* 14:1170603. <https://doi.org/10.3389/fimmu.2023.1170603>
71. Snoderly HT, Boone BA, Bennowitz MF (2019) Neutrophil extracellular traps in breast cancer and beyond: current perspectives on NET stimuli, thrombosis and metastasis, and clinical utility for diagnosis and treatment. *Breast Cancer Res* 21:145. <https://doi.org/10.1186/s13058-019-1237-6>
72. Sadeghi M, Dehnavi S, Jamialahmadi T, Johnston TP, Sahebkar A (2023) Neutrophil extracellular trap: A key player in the pathogenesis of autoimmune diseases. *Int Immunopharmacol* 116:109843. <https://doi.org/10.1016/j.intimp.2023.109843>
73. Scandolaro TB, Panis C (2020) Neutrophil traps, anti-myeloperoxidase antibodies and cancer: Are they linked? *Immunol Lett* 221:33–38. <https://doi.org/10.1016/j.imlet.2020.02.011>
74. Li Y, Wu S, Zhao Y et al (2024) Neutrophil extracellular traps induced by chemotherapy inhibit tumor growth in murine models of colorectal cancer. *J Clin Invest* 134(5):e175031. <https://doi.org/10.1172/JCI175031>
75. Mousset A, Lecorgne E, Bourget I et al (2023) Neutrophil extracellular traps formed during chemotherapy confer treatment resistance via TGF-beta activation. *Cancer Cell* 41:757–775. <https://doi.org/10.1016/j.ccell.2023.03.008>
76. Hinrichs BH, Matthews JD, Siuda D, O'Leary MN, Wolfarth AA, Saedi BJ, Nusrat A, Neish AS (2018) Serum amyloid A1 is an epithelial prorestitutive factor. *Am J Pathol* 188:937–949. <https://doi.org/10.1016/j.ajpath.2017.12.013>
77. Moshkovskii SA (2012) Why do cancer cells produce serum amyloid A acute-phase protein? *Biochemistry (Mosc)* 77:339–341. <https://doi.org/10.1134/S0006297912040037>
78. Abouelasrar Salama S, Gouwy M, Van Damme J, Struyf S (2023) Acute-serum amyloid A and A-SAA-derived peptides as formyl peptide receptor (FPR) 2 ligands. *Front Endocrinol (Lausanne)* 14:1119227. <https://doi.org/10.3389/fendo.2023.1119227>
79. Antelo-Iglesias L, Picallos-Rabina P, Estevez-Souto V, Da Silva-Alvarez S, Collado M (2021) The role of cellular senescence in tissue repair and regeneration. *Mech Ageing Dev* 198:111528. <https://doi.org/10.1016/j.mad.2021.111528>
80. Kowald A, Passos JF, Kirkwood TBL (2020) On the evolution of cellular senescence. *Aging Cell* 19:e13270. <https://doi.org/10.1111/ace1.13270>
81. Fousek K, Horn LA, Palena C (2021) Interleukin-8: A chemokine at the intersection of cancer plasticity, angiogenesis, and immune suppression. *Pharmacol Ther* 219:107692. <https://doi.org/10.1016/j.pharmthera.2020.107692>
82. Jochems F, Thijssen B, De Conti G et al (2021) The cancer SENE-SCopedia: a delineation of cancer cell senescence. *Cell Rep* 36:109441. <https://doi.org/10.1016/j.celrep.2021.109441>

Publisher's Note Springer Nature remains neutral with regard to jurisdictional claims in published maps and institutional affiliations.